Scientific Journal of Impact Factor (SJIF): 5.71
e-ISSN (O): 2348-4470
p-ISSN (P): 2348-6406

International Journal of Advance Engineering and Research Development

Volume 5, Issue 04, April -2018

PREDICTION OF TEMPERATURE OF OVERHEAD CONDUCTORS USING CIGRE THERMODYNAMIC MODEL AND ITS VALIDATION

Mr. Abbas A. Ghadiyali[1], Mr. M.J.Zinzuvadia[2], Mr. P.G. Choksi[3], Dr. G.S.Grewal[4]

[1] *Post-Graduate Student, Mechanical Department, Birla Vishvakarma Mahavidyalaya, Vallabh Vidyanagar, Gujarat, India.*
[2] *Associate Professor, Mechanical Department, Birla Vishvakarma Mahavidyalaya, Vallabh Vidyanagar, Gujarat, India.*
[3] *Assistant Professor, Mechanical Department, Birla Vishvakarma Mahavidyalaya, Vallabh Vidyanagar, Gujarat, India.*
[4] *Dy. Director & Head, MIMD, Electrical Research & Development Organization, Vadodara, Gujarat, India*

ABSTRACT: *In electricity transmission system, the overhead conductors gets heated and cooled due to heat transmission depending on weather parameters at the particular location and the current passing through it. The temperature fluctuations affect the conductors by limiting the maximum current capacity of the conductor, inducing thermal stresses in it which can creates sag of the line, which in turn, reduces the ground clearance and degrading the mechanical properties of the conductor. Therefore, CIGRE (Conseil International des Grands Réseaux Électriques), an organization in the field of high Voltage electricity has proposed a thermodynamic model[1,2] for determining the temperature of the conductor dynamically. This model can be used in DLRS(Dynamic Line Rating Scheme) in which real time monitoring of temperature is done to optimize current according to it. In order to design a dynamic rating scheme, utilities need to know what is the accuracy of the thermodynamic model of the transmission line. In present study, the CIGRE model is analyzed with the help of Matlab software by calculating the hourly temperature of ACSR Zebra conductor and the results are validated by determining the temperature of an actual transmission line.*

Keyword : - *CIGRE thermodynamic model, thermal rating, conductor temperature, dynamic line rating, tranmission line temperature.*

I. INTRODUCTION:

The maximum current capacity of most transmission lines (I_{max}) is limited by a maximum temperature (T_{max}) that the line can reach. Beyond this temperature, the maximum sag of the line can be exceeded and/or degra-dation of the mechanical properties of the conductors can occur [3]. Aside from T_{max}, I_{max} depends on the weather conditions. For example, on a cool day it would take a higher current to warm up the line to T_{max} than during a warm day. To rate a transmission line (i.e. to calculate I_{max} for a given line), most transmission system operators split the year into seasons which have fixed (i.e. static) weather conditions [4]. These conditions are usually conservative and therefore rarely observed. This has the consequence that the line is operated most of the time with a value of Imax which is lower than the real one. To make use of the "remaining" current capacity, it has been proposed to operate the transmission lines under a Dynamic Line Rating Scheme (DLRS) [5, 6, 7, 8]. In this scheme the real weather conditions (or the weather predictions) are used to calculate I_{max} and, therefore, its value is not fixed but changes continuously. Many transmission system operators are pursuing programs to implement a DLRS [9, 10, 11]. This is especially the case in Europe where the increasing international energy flows and the decentralized energy production require a higher transmission capacity of the network [10].

An accurate line temperature model lies at the heart of a DLRS since it allows to calculate I_{max} for a given T_{max} and a set of ambient conditions. Then, one of the first steps to design a specific DLRS is to determine the accuracy of the line temperature model. There has been a lot of work on line temperature modeling [12, 13, 14, 15, 16, 17, 1] as well as in laboratory tests of these models (e.g. response of the line temperature upon current steps) [18, 19], but there is not much work in the determination of the accuracy of these models under realistic operational conditions. In [20] an electrical current was applied to an idle transmission line while the line temperature and weather conditions were monitored. Then, the data from 15 min periods was averaged and a static model (see next section) was used to calculate the line temperature. In [21] two ACSR conductors were mounted in an outdoor setup and monitored every 5 minutes. Air temperature and wind speed were monitored (this last one using a cup anemometer with a threshold velocity of 0.22 m/s), and the solar radiation was assumed to be equal to the theoretical clear sky value. This study reported a precision of the model of 3°C for conductor temperatures below 150°C, and of 24°C for conductor temperatures above 150°C (i.e. at high electrical currents). More recently, in [22] a two ACSR lines were mounted in an outdoors test setup, and the current through them was controlled such that the core of the line remained at 80°C.

In the present study, an algorithm is developed in MATLAB software to determine the temperature of the conductor by considering the various heat transfer taking place at the location of particular transmission line. The algorithm is based on CIGRE thermodynamic model which gives information and emperical formulas of various heat transfer like magnetic heating, joule heating, solar heating, wind cooling and radiative cooling. The algorithm needs various input parameters like latitude of the conductor location, wind velocity, ambient temperature, initial temperature of the transmission line, wind direction, clearness ratio, humidity, day number and current. The input parameters are given hourly and the algorithm will give hourly conductor temperature for the particular day. The algorithm is specifically for ACSR(Zebra) conductor and it can be expanded to include all the types of conductor. The algorithm can be used in DLRS if real time sensors are used for input parameters so that it will give real time conductor temperature and the optimum current.

The results obtained for the particular day were than validated by measuring an actual 220 KV transmission line(Karamsad-Mogar2)using ACSR(Zebra) at Vitthal Udhyognagar near Anand, Gujarat. The temperature were measured hourly using an Infrared Thermal Imager Camera.

II. MEASUREMENT DETAILS:

The actual measurement of high voltage transmission line was performed on 220 KV Karamsad-Mogar2 line near Vitthal Udyognagar, Anand from 8AM to 7PM hourly on 11th February, 2018. The conductor type was ACSR (Zebra). The transmission line height at the spot of measurement was 10 m. The weather parameters for the particular day was noted down during measurement. The wind velocity was measured with the help of vane anemometer at the height of transmission line, ambient temperature from thermocouple, humidity from hygrometer and wind direction from weather forecasting sites. The hourly current data was taken from Karamsad Substation where the line culminates. The temperature of the conductor was measured with the help of TH7800 thermal infrared camera. The conductor design data were taken from the GETCO website. All the above values were measured or collected hourly.

Figure 1: *Anemometer*

Figure 2: *Hygrometer*

III. THE CIGRE MODEL[1]:

If the conductor is assumed to be one-dimensional and homogeneous, and if the weather conditions are constant along the line (so that there are no temperature gradients along the line), the heat equation for the conductor is:

$$\rho . C . \frac{dT}{dt} = \Delta Q$$

where ρ is the linear mass-density of the line, C the specific heat of the line material, T the surface temperature of the line, t the time and ΔP the net energy flowing to the line per unit length and unit time.
The net heat transfer is given by,

$$\Delta Q = Q_j + Q_m + Q_s + Q_i - Q_c - Q_r - Q_w$$

where, Q_j is the Joule heating, Q_s, the solar heating, Q_m the magnetic heating, Q_i the corona heating, Q_c the convective cooling, Q_r the radiative cooling and Q_w the evaporative cooling.

The corona heating can be significant at times of high humidity and high wind speeds, but it is normally irrelevant for rating purposes due to the fact that convective effects at that times are much more important.

The heat loss due to evaporation can have a major effect on the temperature of a conductor, but in most thermal rating calculations it is ignored for being rare that the entire line will be wet and the difficulty of assessment. Safe values without considering this effect are preferred, and therefore:

$$\Delta Q = Q_j + Q_m + Q_s - Q_c - Q_r$$

A. **Joule Heating:**

Joule heating refers to the energy generated by current flow through the conductor. It takes into account the pure direct current resistance and the "skin effect" (the increase of current density towards the surface of the conductor) when alternating currents (ac) are used.

The Joule heat gain per unit length for conductors carrying direct current is found from:

$$Q_j = k_{sk} . I^2 \cdot R_{dc}[1+\alpha(T_{av}-20)]$$

where, k_{sk} is skin effect factor, I is the total direct current (A) and R_{dc} the direct current resistance per unit length (Ω/m), which depends on the resistivity of the materials ρ (Ω·m) at the temperature considered, the cross-sectional area A (m^2) and the conductor temp T(°C).

The temperature of the line is higher in its interior [26, 27, 23] so, strictly speaking, the temperature used in above eqn, should not be the surface temperature T but the cross sectional average of the line temperature. The error on P_J incurred by using T instead of the average conductor temperature, was observed to be approximately 1.5% when the line surface temperature reached 80°C under normal convective cooling conditions for a similar AAAC [23].

This error is expected to be much smaller in the present study though, since the typical currents in the conductors are smaller than the ones used in [23].

With alternating current, the resistance of a conductor increases due to the migration of the current towards the surface of the conductor, a phenomenon known as "skin effect".

The direct current resistance per unit length can be obtained as described in the previous section for the desired temperature. The skin effect factor increases with increasing conductor diameter and with increasing frequency. It is usually less than 1.02 for the normal range of conductor diameters and with commercial frequencies, but could be as much as 1.08 for larger conductors (diameters greater than 45 mm).

Analytical values for the skin effect factor can be calculated using Bessel functions which we have included in the algorithm.

B. Magnetic heating:

In the case of a steel-cored conductor, such as aluminum-conductor steel-reinforced (ACSR), the axial alternating magnetic flux produced by the spiraling conductor layers causes heating in the steel core, P_{core} and heating due to redistribution of the current densities in the layers of the non-ferrous wires, P_{redis}, known as the transformer effect. These magnetic effects may be considerable for certain conductors, although for the majority of the cases in transmission lines they can be considered negligible. The total magnetic heat gain per unit length is the sum of both power losses:

$$Q_m = Q_{core} + Q_{redis}$$

C. Solar Heating:

The solar heat gain per unit length by a conductor, Q_s (W/m), is directly proportional to the outer diameter of the conductor, D (m), the absorptivity of the surface of the conductor, α_s, and the global radiation intensity I_t (W/m2):

$$Qs = \alpha_s \,.\, D \,.\, I_t$$

where,
α_s = absorption coefficient of the line
D = line diameter, m
I_t = Effective Solar radiation, W/m^2

The value of α_s varies from around 0.2 for a bright new conductor to around 0.9 for a weathered conductor in an industrial environment. A new conductor in a heavy industrial environment weathers to around α_s = 0.5 after about one month's exposure, and to around α_s = 0.9 after about one year. The rate of weathering is slower in rural areas. It is not easy to measure the absorptivity accurately. The recommended methods are either determining the emissivity of the conductor, by measuring samples and then estimating absorptivity to be slightly higher than this value (0.1 – 0.2 higher), or using a default absorptivity of no less than 0.8. Conductor surface treatments may provide different values.

Devices for measuring global radiation intensity are relatively inexpensive and reliable, and can be easily used for line monitoring systems, as they can provide measurements of the mean global radiation intensity for a period of time for the dynamic thermal rating calculations. But there are some considerations that have to be noted.

The global radiation received by the conductor is not necessarily the same at all points along the line. It depends on the location, and important differences may arise due to different orientation, sheltered areas, reflectance from ground, etc. The variability with time is also not the same at all points along the line.

The global radiation intensity, I_t, is a combination of the direct solar radiation on a surface normal to the Sun's beam, I_d, the diffuse sky radiation to a horizontal surface, I_b, and the incident radiation reflected from the ground or albedo, F. The formula for the total solar power received per unit length of the conductor (W/m) is given by,

$$I_t = I_B\left(\sin(\eta) + \frac{\pi}{2} \times F \times \sin(H_s)\right) + I_d(1 + \frac{\pi}{2} \times F)$$

where,
η = angle of solar beam w.r.t. axis of the conductor, degrees
H_s = solar Hour angle, degrees
An equation to calculate the direct solar radiation at sea level,

$$I_b = N_s \times \frac{1280 \times sin(H_s)}{sin(H_s) + 0.314}$$

where, N_s is a clearness ratio, having the value of 1.0 for the standard atmosphere, 0.8 to 1.2 for clear skies with decreasing amounts of dust and aerosols, 0.5 for an industrial atmosphere and less than 0.5 for a cloudy or overcast sky. With thick cloud, N_s = 0.
H_s is the solar altitude, given by:

$$H_s = \arcsin(\sin(\varphi) \cdot \sin(\delta_s) + \cos(\varphi) \cdot \cos(\delta_s) \cdot \cos(Z))$$

where,
φ = latitude, *degrees*
$\delta_s = declination = 23.3 \cdot \sin\left(\frac{2\pi \cdot (284+N^*)}{365}\right)$, *degrees*
The declination of the sun can be defined as the angle between the equator and a line drawn from the centre of the earth to the centre of the sun.
Here,
N^* = day of the year(0 to 365)
Z = hour angle of the sun = 15(12 - time), time in hours from 0 to 24
The solar hour angle decreases by 15 degrees for every hour from zero at solar noon. To obtain solar time, add 4 minutes per degree of longitude east of standard time, or subtract 4 minutes per degree west of standard time. There is also a small time correction, not exceeding 16 minutes, for perturbations in the earth's rotation.

I_d is the diffuse solar radiation intensity (W/m^2). There is a correlation between direct radiation I_b and diffuse radiation, I_d, as clouds cause both a reduction in and an increase in I_d. An equation to calculate the diffuse radiation for all skies is,

$$I_d = (430.5 - 0.3288 \cdot I_B) \cdot \sin(H_s)$$

η is given by,

$$\eta = \arccos[\cos(H_s) \cdot \cos(\gamma_s - \gamma_c)]$$

where,
γ_c = azimuth of the conductor, *degrees*
γ_s = azimuth of the sun = $arcsin\left(\frac{\cos(\delta_s) \cdot \sin(Z)}{\cos(H_s)}\right)$, *degrees*
F is the albedo or reflectance of the ground. The albedo (F) is approximately 0.05 for a water surface (> 30˚), 0.1 for forests, 0.15 for urban areas, 0.2 for soil, grass and crops, 0.3 for sand, 0.4 to 0.6 for ice and 0.6 to 0.8 for snow. The albedo tends to increase as the solar altitude increases.
The residual gain at night can be considered negligible.

D. Convective Cooling:

Convection is almost always the most important factor for cooling overhead conductors, even for still air conditions (zero wind speed). Conductor temperatures can only be high when convective cooling is low. Hence, for thermal rating purposes, the focus is on situations where wind speed is low or zero.

Two types of convection are considered: natural convection, which occurs when wind speed is zero; and forced convection which depends on wind speed and direction relative to the line. At moderate-to-high wind speeds, forced convection dominates and natural convection can be ignored. At low wind speeds, natural convection may have a significant effect, becoming the dominant convection mechanism at very low wind speeds.

Wind variability, even within a single span, makes it very difficult to assess the thermal behavior of overhead lines, particularly at low wind speeds and high current densities. As noted previously, the axial differences in conductor temperature can be very significant, mainly due to wind variability. Therefore, even though the equations to model the local heat transfer are accurate, the behavior of the whole line section or a single span may be different. So, for thermal rating purposes, it is necessary to consider this variability and model the wind properly. It is not simple, and some approaches based on statistical analysis are under development to consider this problem. For example, the concept of "effective wind speed" has been introduced as the perpendicular, laminar wind speed which produces the same cooling effect along an entire section.

The heat transfer from a bare stranded overhead conductor to a surrounding atmosphere is dependent on the coefficient of convective heat transfer, (W/K·m^2). In order to obtain empirical values that can be used in practical situations, the convective heat loss can be expressed as a function of the dimensionless Nusselt number (see nomenclature) as follows:

$$Q_c = \pi \cdot \lambda_f \cdot I \cdot (T_s - T_a) \cdot Nu$$

where λ_f is the thermal conductivity of the air (W/K·m) at T_f the temperature of the film of air in contact with the surface, T_s and T_a are the temperatures of the conductor surface and the air respectively.
For film temperatures up to 300°C the thermal conductivity of the air can be expressed as,

$$\lambda_f = 2.368 \times 10^{-2} + 7.23 \times 10^{-5} \cdot T_f - 2.763 \cdot 10^{-8} \cdot T_f^2$$

where the film temperature is assumed to be $T_f = 0.5(T_s + T_a)$
(i) For wind velocity higher than 0.5 m/s(forced convection),

$$Nu = 0.65\ Re^{0.2} + 0.23\ Re^{0.61}$$

$$Re = 1.644e.10^9\ V\ D\ (T_a + 273 + 0.5(T - T_a))^{-1.78}$$

where Re is the Reynolds number and V the wind speed. The values for A in can be obtained from,

$$A = 0.42 + 0.68 * (\sin(\Phi))^{1.08} \qquad \Phi < 24^o$$

$$A = 0.42 + 0.58 * (\sin(\Phi))^{0.9} \qquad \Phi > 24^o$$

where φ is the angle between the line direction and the wind.

(ii) For the case of zero or negligible wind speed(natural convection),

$$Nu = B(Gr.Pr)^m$$

$$Gr = \frac{D^3(T - T_a)g}{(T_f + 273) \cdot v^2}$$

$$P_r = C \cdot \frac{\mu}{\lambda}$$

$$v = \frac{\mu}{\gamma_a}$$

$$\mu = (17.239 + 4.635 \times 10^{-2} \cdot T_f - 2.03 \times 10^{-5} \cdot T_f^2) \times 10^{-6}$$

$$\gamma_a = \frac{1.293 - 1.525 \times 10^{-4} y + 6.379 \times 10^{-9} y^2}{1 + 0.00367 \cdot T_f}$$

where G_r is the Grashof number, P_r is the Prandtl number, g the gravitational acceleration, C the heat capacity of the air, v the kinematic viscosity of the air, μ the dynamic viscosity of the air, γ the air density and y the altitude of the line above the sea level. B and m in are empirical coefficients which depend on the product of the Grashof and Prandtl numbers, and their values are shown in Table for different ($G_r\ P_r$) ranges.

***Table 1:** Conditions: Product of Gr and Pr values*

	B	M
$10^{-1} <= Gr.Pr < 10^2$	1.02	0.148
$10^2 <= Gr.Pr < 10^4$	0.85	0.188
$10^4 <= Gr.Pr < 10^7$	0.48	0.25
$10^7 <= Gr.Pr < 10^{12}$	0.125	0.333

E. Radiative Cooling:

The net radiative heat loss from a conductor is the total radiative energy transmitted from its surface. It can be divided into two components: the heat radiated to the ground and surroundings, and the heat radiated directly to the sky. Applying the Stefan-Boltzmann law, the heat loss from the conductor due to radiation can be expressed as

$$Q_r = \pi . D . \varepsilon . \sigma_B[(T_s + 273)^4 - (T_a + 273)^4]$$

where σ_B is the Stefan-Boltzmann constant (5.6697 × 10^{-8} W/m^{2}K^4), E is the emissivity of the line, T_{grnd} the temperature of the ground in ^{o}C.
After accounting sky thermal radiation,

$$Q_r = \pi \cdot D \cdot \sigma_B \cdot \varepsilon \frac{(T + 273)^4 - (T_a + 273)^4}{2} + \pi \cdot D \cdot \varepsilon \cdot \frac{\sigma_B (T + 273)^4 - 8.78 \times 10^{-13} (T_a + 273)^{5.852} \cdot R_h^{0.07195}}{2}$$

where R_h is the relative humidity.

IV. RESULTS AND DISCUSSION:

As mentioned above, the measurement were done on 11th February, 2018 on ACSR transmission line(Karamsad-Mogar) at Vitthal Udhyognagar. The parameters of the transmission line are as follows,

Figure 3: *Location of Measurement*

Table 2: Parameters of the transmission line conductor

Parameter	**Value**
Skin Effect Factor, k_{sk}	1.08
Resistivity coefficient, α_{20}	3.6 * 10^-3 Ω m
Resistance, R_{dc}	6.8 * 10^-5 Ω/m
Latitude, Φ	22.5275(Vitthal Udhyognagar)
Ground albedo, F	0.3(sand and grass)
Absorption Coefficient, α_c	0.8
Diameter of the conductor, D(ACSR Zebra)	28.62 mm
Strand diameter, d_s, d_a	3.18, 3.18mm
Azimuth of the conductor, γ_c	90^o
Emissivity of the conductor, ε	0.8
Transmission line height, y	12 m
Specific heat, c_s, c_a	481, 897 J/kg K
Mass, m_s, m_a	0.5119, 1.116 kg/m
Initial temperature of the conductor(At 8:00am)	23^oC

Figure 4: *Thermal Infrared Camera*

The measured values of the conductor temperature are as follows:

Table 3: Measured Values of conductor temperature

Time	**Temperature(^{0}C)**
8:00	21
9:00	28
10:00	28.3
11:00	28.6
12:00	29.9
13:00	31.2
14:00	31
15:00	32
16:00	31.4
17:00	35.2
18:00	34.1
18:30	36.3

Then, the input parameters for the particular day were measured simultaneously. The various parameters like humidity, ambient temperature, wind velocity, wind direction, current are given in the following tables:

Hourly ambient temperature data(^{o}C):

00:00	**01:00**	**02:00**	**03:00**	**04:00**	**05:00**	**06:00**	**07:00**	**08:00**	**09:00**	**10:00**	**11:00**
18	17.78	17.78	17.78	17.25	16.12	15.56	17	21	23	24	26
12:00	**13:00**	**14:00**	**15:00**	**16:00**	**17:00**	**18:00**	**19:00**	**20:00**	**21:00**	**22:00**	**23:00**
29.7	30.6	29.5	30.2	28.2	28.6	25.3	24	22	20	19	18

Hourly Wind Speed data(m/s):

00:00	**01:00**	**02:00**	**03:00**	**04:00**	**05:00**	**06:00**	**07:00**	**08:00**	**09:00**	**10:00**	**11:00**
0.56	0.28	0.3	0.3	0.28	0.56	0.56	0.28	0.5	0.77	1.65	2
12:00	**13:00**	**14:00**	**15:00**	**16:00**	**17:00**	**18:00**	**19:00**	**20:00**	**21:00**	**22:00**	**23:00**
2.75	1.8	2.5	2.5	3	0.8	0.8	1.3	1.12	1.2	0.8	0.9

Hourly Wind Direction data(deg):

00:00	**01:00**	**02:00**	**03:00**	**04:00**	**05:00**	**06:00**	**07:00**	**08:00**	**09:00**	**10:00**	**11:00**
70	20	25	20	20	20	20	20	12	12	15	25
12:00	**13:00**	**14:00**	**15:00**	**16:00**	**17:00**	**18:00**	**19:00**	**20:00**	**21:00**	**22:00**	**23:00**
25	25	25	20	20	20	15	12	60	45	55	60

Hourly relative humidity data(R_h):

00:00	**01:00**	**02:00**	**03:00**	**04:00**	**05:00**	**06:00**	**07:00**	**08:00**	**09:00**	**10:00**	**11:00**
0.86	0.91	0.96	0.96	0.92	0.9	0.85	0.81	0.64	0.64	0.6	0.55
12:00	**13:00**	**14:00**	**15:00**	**16:00**	**17:00**	**18:00**	**19:00**	**20:00**	**21:00**	**22:00**	**23:00**
0.48	0.38	0.35	0.41	0.4	0.46	0.49	0.4	0.47	0.56	0.65	0.75

Hourly current data(A):

00:00	**01:00**	**02:00**	**03:00**	**04:00**	**05:00**	**06:00**	**07:00**	**08:00**	**09:00**	**10:00**	**11:00**
114	128.4	135.6	125.4	124.2	133.8	120.6	135.6	147	153	164.4	162.6
12:00	**13:00**	**14:00**	**15:00**	**16:00**	**17:00**	**18:00**	**19:00**	**20:00**	**21:00**	**22:00**	**23:00**
163.8	145.2	156.6	156.6	149.4	125.4	132.6	109.2	117	114	119.4	115.8

Hourly clearness ratio data:

00:00	**01:00**	**02:00**	**03:00**	**04:00**	**05:00**	**06:00**	**07:00**	**08:00**	**09:00**	**10:00**	**11:00**
-	-	-	-	-	-	-	0.85	0.8	0.9	0.9	0.9
12:00	**13:00**	**14:00**	**15:00**	**16:00**	**17:00**	**18:00**	**19:00**	**20:00**	**21:00**	**22:00**	**23:00**
0.8	0.67	0.9	0.85	0.95	0.5	0.5	-	-	-	-	-

All the above parameters were fed into MATLAB program to generate the simulated results of conductor temperature. The calculation is done by taking the input parameters linearly for 1 hour. The results of the simulation are as follows:

Table 4: Simulated values in MATLAB

Time	Temperature(^oC)	Time	Temperature(^oC)
00:00	25.09	12:00	26.08
01:00	24.13	13:00	27.66
02:00	23.46	14:00	28.92
03:00	22.81	15:00	29.92
04:00	22.21	16:00	30.63
05:00	21.61	17:00	30.69
06:00	20.93	18:00	30.66
07:00	20.25	19:00	30.28
08:00	23	20:00	29.9
09:00	23.32	21:00	28.67
10:00	24	22:00	27.41
11:00	24.92	23:00	26.26

The simulated results were compared with the measured values of temperature conductor which is given as follows:

Table 5: Comparison between measured and simulated values

Time	Measured Temp(^0C)	Simulated Temp(^0C)	Difference
8:00	23	23	0
9:00	28	23.32	4.68
10:00	28.3	24	4.3
11:00	28.6	24.92	3.68
12:00	29.9	26.08	3.82
13:00	31.2	27.66	3.54
14:00	31	28.92	2.08
15:00	32	29.92	2.08
16:00	31.4	30.63	0.77
17:00	31.5	30.69	0.81
18:00	31.6	30.66	0.94
18:30	30.25	30.28	-0.03

The comparison of the simulated and measured values are plotted in the following graph. The temperature values are in ^oC and the time is in hours from 8:00 AM to 7:00 PM next day. The simulated values are for 24 hours while the measured valuess are for 12 hours.

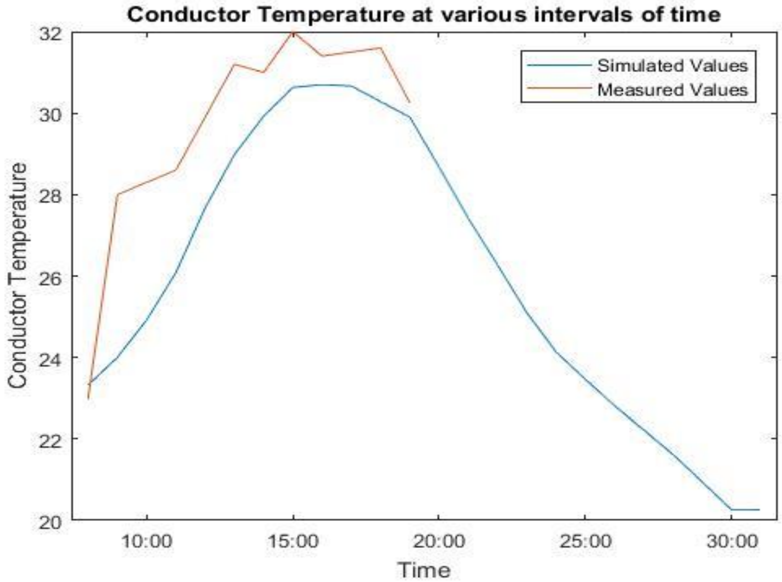

Figure 5: Comparison between measured and simulated values of conductor temperature

V. CONCLUSION:

From the above study, a comparison between the simulated and measured temperature of transmission line conductor was done according to CIGRE thermodynamic model. A variation of +/- 3°C(+/-2%) was observed. There are some inaccuracies involved like human errors, instrument errors, and errors in measurement of weather parameters. In addition, we have measured the surface temperature of conductor, although there is a variation in core and surface temperature in a conductor. Though, the difference is less at temperature less than 80°C[23]. The MATLAB program can be used to predict the hourly temperature of conductor of transmission line for any day of the year if we have necessary forecasted weather data like wind velocity, ambient temperature, wind direction, relative humidity, according to CIGRE thermodynamic model.

Further, by improving the MATLAB program, it can be used in conjunction with real time sensors to calculate the real time values of the conductor temperature and with the help of it, the optimum current can be calculated for DLRS(Dynamic Line Rating Scheme). In addition, a slight change can be done in the MATLAB code to determine temperature for other types of conductor like AAAC, AAC, ACAR, etc.

VI. ACKNOWLEDGEMENT:

The research was financially sponsored by Electrical Research & Development Organization (ERDA), Vadodara. We are thankful to GETCO and Karamsad Substation for giving us necessary permission and data for carrying out this research.

REFERENCES

[1] WG B2.43, “Guide for Thermal Rating Calculations of Overhead Lines,” Tech. Rep. 601, Cigr`e, International Council on Large Electric Systems, 2014.

[2] WG 22.12, “Thermal behaviour of overhead conductors,” Tech. Rep. 207, Cigr`e, International Council on Large Electric Systems, 2002.

[3] J. Kaufman, Properties of Aluminum Alloys. The Aluminum Associa-tion, 1999.

[4] WG B2.12, “Guide for Selection of Weather Parameters for Bare Overhead Conductor Ratings,” Tech. Rep. 299, Cigr`e, International Council on Large Electric Systems, 2006.

[5] M. Davis, “A New Thermal Rating Approach: the Real Time Thermal Rating System for Strategic Overhead Conductor Transmission Lines, Part I, General Description and Justification of the Real Time Thermal Rating System,” Power Apparatus and Systems, IEEE Transactions on, vol. PAS-96, no. 3, pp. 803–809, 1977.

[6] G. Ramon, "Dynamic Thermal Line Rating, Summary and Status of the State-of-the-Art Technology," IEEE Transactions on Power Delivery, vol. PWRD-2, no. 3, pp. 851–858, 1987. Prepared by a Task Force of the Working Group on Calculation of Bare Overhead Conductor Temperatures.

[7] D. Douglass and A. Edris, "Real-Time Monitoring and Dynamic Thermal Rating of Power Transmission Circuits," IEEE Transactions on Power Delivery, vol. 11, no. 3, pp. 1407–1418, 1996.

[8] J. Hosek, P. Musilek, E. Lozowski, and P. Pytlak, "Effect of Time Resolution of Meteorological Inputs on Dynamic Thermal Rating Calculations," IET Generation, Transmission & Distribution, vol. 5, no. 9, pp. 941–947, 2011.

[9] Energy Sector Planning and Analysis (ESPA), W. Wang, and S. Pinter, "Dynamic Line Rating Systems for Transmission Lines," tech. rep., ESPA, april 2014.

[10] W. Winter, K. Elkington, G. Bareux, and J. Kostevc, "Pushing the Limits," IEEE Power & Energy Magazine, vol. 13, no. 1, pp. 60–74, 2015.

[11] ENTSOE, "Dynamic Line Rating for Overhead Lines - V6," tech. rep., European Network of Transmission System Operators for Electricity, March 2015.

[12] V. Morgan, "The thermal rating of overhead-line conductors Part I. The steady-state thermal model," Electric Power Systems Research, vol. 5, pp. 119–139, 1982.

[13] W. Black and W. Byrd, "Real-time ampacity model for overhead lines," IEEE Transactions on Power Apparatus and Systems, vol. PAS-102, no. 7, pp. 2289–2293, 1983.

[14] S. Foss, S. Lin, and R. Fernandes, "Dynamic Thermal Line Ratings / Part I/ Dynamic Ampacity Rating Algorithm," Power Apparatus and Systems, vol. 00, no. 6, pp. 1858–1864, 1983.

[15] W. Black and R. Rehberg, "Simplified model for steady state and real-time ampacity of overhead conductors," IEEE Transactions on Power Apparatus and Systems, vol. PAS-104, no. 10, pp. 2942–2953, 1985.

[16] IEC technical committee 7, "Overhead electrical conductors- Calcula-tion methods for stranded bare conductors," tech. rep., International Electrotechnical Commission.

[17] "IEEE standard for calculating the current-temperature of bare over-head conductors," tech. rep., IEEE Power Engineering Society.

[18] S. Foss, S. Lin, and R. Carberry, "Significance of the Conductor Radial Temperature Gradient Within a Dynamic Line Rating Methodology," IEEE Transactions on Power Delivery, vol. PWRD-2, no. 2, pp. 502– 511, 1987.

[19] S. Lin, "Heat transfer in an overhead electrical conductor," Int. J. Heat Mass Transfer, vol. 35, no. 4, pp. 795–801, 1992.

[20] W. Chisholm and J. Barrett, "Ampacity studies on 49°c-rated trans-mission line," IEEE Transactions on Power Delivery, vol. 4, no. 2, pp. 1476–1491, 1989.

[21] S. L. Chen, W. Z. Black, and H. W. Loard, "High-temperature am-pacity model for overhead conductors," IEEE Transactions on Power Delivery, vol. 17, no. 4, pp. 1136–1141, 2002.

[22] V. Djurica, G. Lakota, M. Maksi˘c, J. Kosma˘c, and J. Kostevc, "A reference testing site for evaluation of dynamic thermal rating algo-rithm uncertainties in the operation of transmission power lines," in The 19th International Symposium on High Voltage Engineering, Pilsen, Czech Republic, August 2015.

[23] J. Rodriguez Alvarez and C. M. Franck, "Radial thermal conducti-vity of all-aluminum alloy conductors," IEEE Transactions on Power Delivery, vol. 30, no. 4, pp. 1983–1990, 2015.

[24] D. Douglass, "Radial and Axial Temperate Gradients in Bare Stranded Conductor," IEEE Transactions on Power Delivery, vol. 1, no. 2, pp. 7– 15, 1986.

[25] V. Morgan and R. Findlay, “Effects of axial tension and reduced air pressure on the radial thermal conductivity of a stranded conductor,” IEEE Transactions on Power Delivery, vol. 8, pp. 553–558, 1993.

[26] “Aeronet - aerosol robotic network.” http://aeronet.gsfc.nasa.gov/, Au-gust 2015.

[27] D. Mayers, Solar radiation, Practical *Modeling for Renewable Energy Applications. Energy and the Environment, CRC Press, 2013.*

